

Lazarus [Phys. Rev. **76**, 545 (1949)] and discussed by H. B. Huntington [in *Solid State Physics*, edited by F. Seitz and D. Turnbull (Academic, New York, 1958), Vol. 7, p. 234].

⁹W. D. Wilson and R. A. Johnson, Phys. Rev. B **1**, 3510 (1970).

¹⁰R. A. Johnson and W. D. Wilson, in *Interatomic*

Potentials and Simulation of Lattice Defects, edited by P. C. Gehlen, J. R. Beeler, Jr., and R. I. Jaffee (Plenum, New York, 1972), p. 301.

¹¹F. C. Von der Lage and H. A. Bethe, Phys. Rev. **71**, 612 (1947).

¹²K. Huang, Proc. Roy. Soc. (London) **A266**, 1 (1962).

Cyclotron Resonance in Tellurium

M. v. Ortenberg* and Kenneth J. Button

Francis Bitter National Magnet Laboratory, † Massachusetts Institute of Technology, Cambridge, Massachusetts 02139

and

G. Landwehr and D. Fischer

Physikalisches Institut der Universität, ‡ Würzburg, Germany

(Received 12 April 1972)

A study of the temperature dependence of the position, shape, and width of the submillimeter cyclotron-resonance absorption line has provided data which have been compared with the predictions of several theoretical models. The data favor the valence-band structure of tellurium as proposed by Weiler. This shows that the Landau levels are not parallel in the k_x direction. It also shows that the transitions between Landau levels at low temperature occur at the valence-band maximum on the camel back and not at $k_x=0$. Previous experiments, two other theoretical models, and previous attempts to fit band parameters are reviewed and evaluated.

I. INTRODUCTION

The structure of the upper valence band of tellurium has a camel-back shape for its $E(k_x)$ dependence as first proposed by Betbeder-Matibet and Hulin¹ and rigorously derived by Doi, Nakao, and Kamimura²⁻⁴ using the $\vec{k} \cdot \vec{p}$ method. Attempts to determine the valence-band parameters of the camel-back model have generated a number of different theoretical approaches which differ in their higher-order terms and also in the values of their constants. It was not possible to decide from the available experimental data which of the models is the most realistic.

Therefore, the principal objective of the present experiments was to carry out a careful study of submillimeter cyclotron resonance as a function of temperature and to compare the results with the temperature dependence predicted by each of the models. We measured position, width, and shape of the cyclotron-resonance line at temperatures from a few degrees to 120 K. Consistent results could only be obtained by eliminating extraneous influences which had been present in previous experiments⁵⁻¹² owing to specimens of insufficient purity. So we selected very pure, Czochralski-grown specimens in which impurity absorption and changes in the transmission, caused by a variation

of the refractive index with the magnetic field, are practically absent and therefore do not interfere with the study of the cyclotron absorption line.

Our spectrum therefore consisted of a single absorption line when the magnetic field was parallel to the trigonal axis of the crystal. Thus we were able to obtain precise data and to compare these data with the theoretical predictions. The additional details of the experimental conditions and results are described in Secs. II and III.

The comparison of our low-temperature experimental results with three theoretical approaches described in Secs. IV and V does not favor model W2⁹ nearly as well as model W1.¹³ We conclude that for the magnetic field parallel to the c axis of the crystal the energy separation of the Landau levels is not constant, but a function of the wave vector parallel to the magnetic field; i. e., the Landau levels are not equidistant as a function of k_x . Both model W1 and model J¹⁰ predict non-equidistant Landau levels but the quantitative comparison favors model W1, which seems to be the most realistic one so far. However, further improvements in the theoretical approach are desirable.

From our detailed calculations we can also assert that the transitions between Landau levels at low temperatures occur at the valence-band maxi-

mum on the camel back and not at $k_z=0$. All these models predict this if reasonable values of the damping constant are used. These two conclusions are discussed in Secs. VI and VII.

II. SURVEY OF EXPERIMENT

We measured the cyclotron resonance of holes in p -type tellurium at two submillimeter wavelengths by using the 220- μm radiation from a water-vapor laser and the 337- μm radiation from an HCN laser. The continuous-wave output power was a few milliwatts. The radiation was guided to the specimen through hollow brass light pipes, $\frac{1}{2}$ and 1 in. in diameter as described previously.¹⁴ The specimen was situated at the center of a water-cooled copper solenoid magnet. The temperature of the specimen could be changed continuously from about 5 K to room temperature by adjusting the flow of liquid helium around the sample section of the light pipe, by adjusting the pressure of the helium exchange gas in the light pipe, and by adjusting the electric current supplied to a heater near the specimen. A carbon resistance thermometer was used to determine the temperature. The laser radiation, chopped at 15 Hz, was detected after it passed through the specimen by using a germanium or silicon bolometer operated at 4.2 and 1.4 K, respectively. Phase-sensitive amplification was used in connection with a ratio device to compensate long-time drift in the laser intensity.

The radiation from the lasers was unpolarized because it was coupled out through a small hole in the center of a 3-in.-diameter laser mirror. We could produce circularly polarized radiation by means of a linear polarizing grid and a quarter-wave quartz plate placed on the specimen. Whereas the degree of polarization of the linear polarizers was about 100%, the circular polarization was sensitively affected by the angle of incidence on the quartz plate. Radiation reflected from the wall of the light pipe could seriously change the degree of circular polarization. We achieved an optimum polarization of about 90% depending on the alignment and mode operation of the laser.

All of our pure samples originated from the same tellurium single crystal "R Te 14" grown by the Czochralski method, which is superior to the Bridgman method for pulling tellurium because the dislocation density is much smaller. The hole concentration $p = 4 \times 10^{13} \text{ cm}^{-3}$ and conductivity $\sigma = 0.638 (\Omega \text{ cm})^{-1}$ were measured at 4.2 K in the end pieces of the original ingot where the largest impurity concentration is usually found.

The influence of strain has been blamed for observed shifts in the cyclotron-resonance line.¹² We tried to eliminate this by using specimens of different thicknesses that were cut, etched, and

polished by different standard methods as listed in Table I. The final entry in Table I describes a typical specimen that is less pure than our pure ingot which we used for a comparison in Fig. 1. Its free-carrier concentration was an order of magnitude higher, $p = 3 \times 10^{14} \text{ cm}^{-3}$.

III. EXPERIMENTAL RESULTS

A. Present Results

It was the objective of this work to make careful observations of the temperature dependence of the cyclotron-resonance absorption position (effective mass) for comparison with the predictions of three recent models, as shown in Figs. 2, 3, and 4, for example. Note that there is a variation of magnetic field intensity at the absorption maximum of only 2% between 5 and 60 K. The solid curves of Fig. 1 represent typical recordings of the cyclotron resonance from which the points in subsequent figures were obtained. In order to show to what extent cyclotron-resonance spectra can be obscured by extraneous effects such as impurity absorption and optical interference, another spectrum is plotted in Fig. 1 (dotted line). The free-carrier concentration is only one order of magnitude higher than in our pure specimens.

Each of the specimens cut from the pure ingot R Te 14, with a hole concentration of $p < 4 \times 10^{13} \text{ cm}^{-3}$ measured in high fields at helium temperatures, provided a spectrum containing only the cyclotron-resonance line. We did not see the impurity-absorption line reported earlier^{6,10-12} even at temperatures as low as 5 K. We also did not see the splitting reported by Dreybrodt *et al.*⁹ nor did we see the two temperature-dependent transitions reported by Yoshizaki and Tanaka.¹⁰ We also did not see the shift of the resonance that Renk¹² attributed to stress. Indeed, the absence of the extraneous effects that appear in the previous experiments leads us to believe that pure specimens are necessary to obtain sufficiently accurate data for the purposes shown in Figs. 2, 3, and 4, and this belief is confirmed in Figs. 5, 6, and 7 for the longer radiation wavelength of 337 μm .

TABLE I. List of specimens.

	Specimen	Preparation	Thickness (μm)
R Te 14	I parallel	Acid saw, etch polished	1500
	I nonparallel	Acid saw, etch polished	1500
	III	Acid saw, etch polished	4000
	V	Spark cutting, etched	4500
	VII	Acid saw, etch polished	4650
	VIII	Acid saw, etch polished, broken into pieces	700
H W Te 27 IV		Acid saw, etch polished	2200

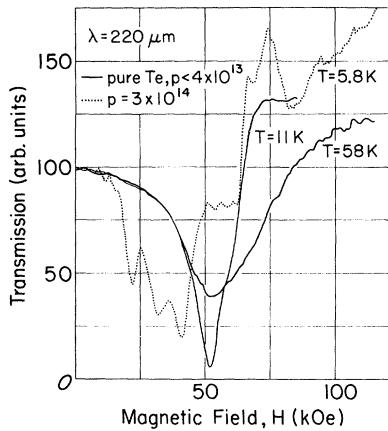


FIG. 1. Transmission of 220- μm radiation through tellurium as function of the magnetic field. The pure specimen (*R Te 14/V*), 4.5 mm thick, shows a single cyclotron-resonance absorption line whereas the less pure specimen (*H W Te 27/IV*), 2.2 mm thick, shows other effects.

B. Previous Results

All previous cyclotron-resonance measurements in Te for $\vec{B} \parallel \vec{c}$ ⁵⁻⁷ showed, so far, a detailed multi-line structure. Some of the low-field lines are evidently impurity transitions because of their tem-

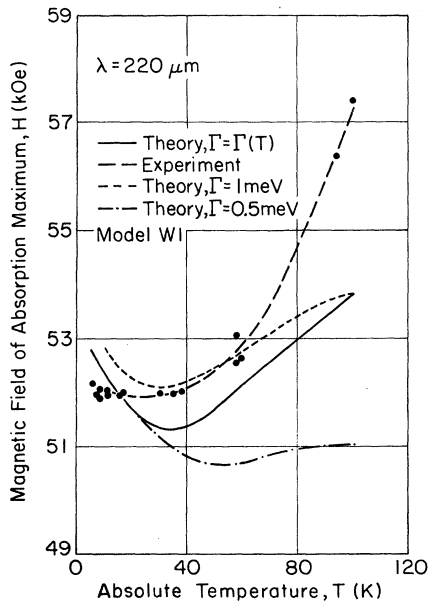


FIG. 2. Magnetic field of absorption maximum of 220- μm radiation in a specimen of pure tellurium as a function of temperature. Theory based on model W1 involving nonparallel Landau levels. The best fit occurs at low temperature. The attempt to fit with $\Gamma = \Gamma(T)$ improved the comparison, but the models are not satisfactory at high temperatures.

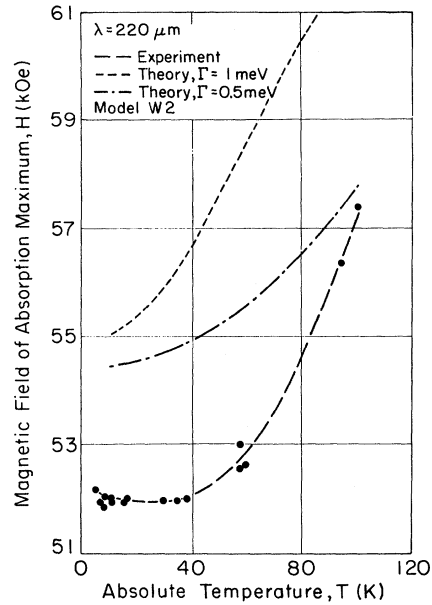


FIG. 3. Experimental data from the pure specimens show a broad minimum (lower left), but this theoretical model involving parallel Landau levels does not predict the minimum.

perature dependence.⁹ The splitting of the cyclotron-resonance line as found by Dreybrodt *et al.*,⁹ however, is more likely explained by interference effects as observed by Button *et al.*¹⁵ in CdS and interpreted by Cronburg and Lax.¹⁶ This effect has

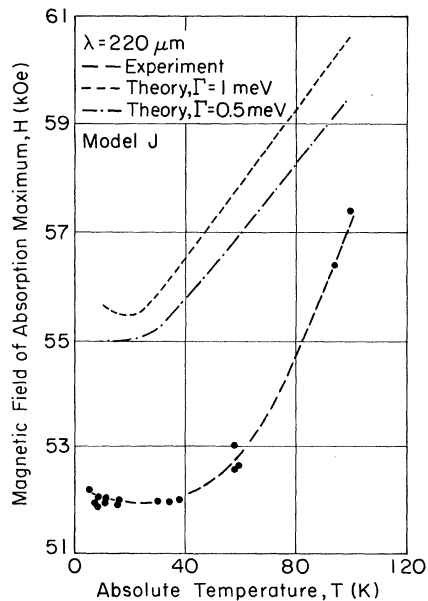


FIG. 4. Comparison of experimental measurements at wavelength of 220 μm with predictions of model J based on nonparallel Landau levels.

only been observed in those of our samples showing a nonmonotonic increase in transmission when cooling down. This indicates that small variations of the refractive index by a change of carrier concentration produce considerable changes in the transmission. We assume that for a theoretical simulation of the interference effects in our samples we have not only to consider the partial degree of polarization by the light pipes¹⁶ but also the variation of the sample thickness. The large refractive index in Te produces for a few microns variation in the sample thickness already considerable changes in the transmission as our computations showed.

Renk¹² observed a change in transmission and line position after rough handling of the sample. He interpreted this effect as produced by strain effects. Our measurements on pure samples, however, showed no variations of the line position independent of preparation and handling of the specimen even for deliberately broken crystals. This is not surprising because strain effects more likely produce a shift of the band edge, as found by Fischer and Grosse,¹⁷ than a change of the effective mass. The change in transmission of the sample after rough handling as found by Renk¹² should rather be explained by a change of sample geometry and thus by interference effects than by a change of the band parameters.

It is probable that the same effect caused the pe-

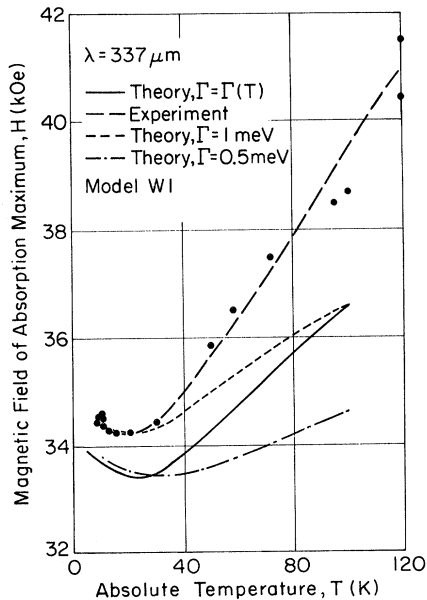


FIG. 5. Best fit between experimental measurements at 337 μm and model W1 occurs at temperatures below 30 K. The attempt to fit with $\Gamma = \Gamma(T)$ improved the comparison somewhat, but the models are not satisfactory at high temperatures.

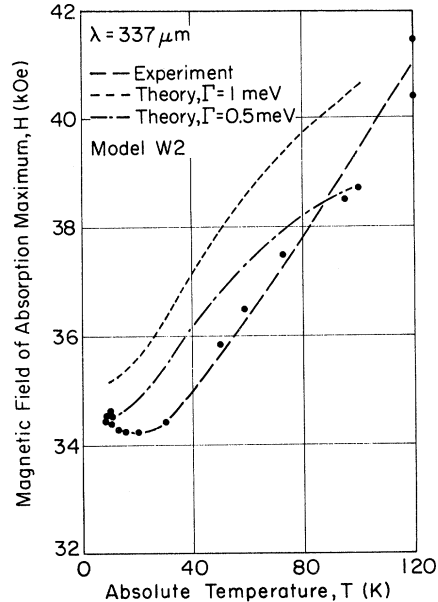


FIG. 6. Minimum in the experimental data at low temperature is not predicted by this model which involves parallel Landau levels.

culiar cyclotron-resonance spectrum for $\vec{B} \parallel \vec{c}$ reported earlier.⁷

IV. BAND-STRUCTURE MODELS OF TELLURIUM

Betbeder-Matibet and Hulin¹ made a semiempirical approach to the band structure of Te which was confirmed later by the straightforward application of the $\vec{k} \cdot \vec{p}$ method by Doi, Nakao, and Kamimura.² Successively different trials were made to fit the various parameters of the model by comparison with cyclotron-resonance experiments.^{3,4,8-10} For that purpose the energy levels in the presence of a magnetic field of the different models have been calculated independently by Weiler¹³ and Nakao *et al.*⁴ for the two favorite crystal orientations relative to the magnetic field, and by Bangert and Ortenberg¹⁸ for any crystal orientation.

Three of these models, W1,¹³ W2,⁹ and J¹⁰ have been chosen to be discussed here. The H_4 energy band E can be expressed as

$$E = a + bk_z^2 + ck_1^2 + dk_1^4 + ek_z^2 k_1^2 + [(a + fk_1^2 + gk_1^4) + hk_z^2]^{1/2}, \quad (1)$$

where the coefficients, or band parameters, are given in Table II for each model. The main difference among these models lies in the k_z dependence. Model W1 seems to have the most general functional dependence because it includes the important $k_z^2 k_1^2$ term. In W2 and J this term is not considered. In general, all of the coefficients of each of the models are temperature dependent. As

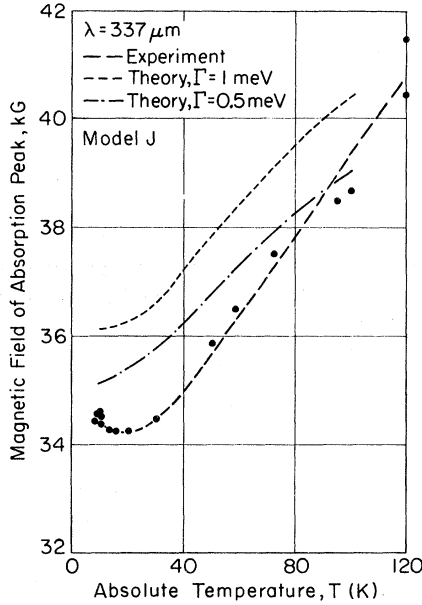


FIG. 7. Distinct minimum at low temperature in the experimental data taken at a wavelength of $337 \mu\text{m}$ is not predicted by model J for these choices of damping parameter Γ .

Gspan *et al.*¹⁹ have shown, the atomic distances in the Te lattice change by about 0.25% with the temperature increasing from 0 to 50 K and by about 1.2% with the temperature increasing up to 300 K. Shubnikov-de Haas measurements under hydrostatic pressure by Anzin *et al.*^{20,21} revealed that a 0.25% estimated change of the atomic distances already affects the band-structure parameters. The most evident interpretation of their measurements produces a depth variation of the minimum in the camel back. Such a change in the camel back with temperature should produce pronounced shifts in the cyclotron-resonance spectrum for the magnetic field perpendicular to the trigonal axis of the crystal. Our measurements for this orientation up to 60 K do not show, however, any shift of line position. Therefore such a temperature variation of the band-structure parameters will be

neglected in our calculations, and all of the parameters are treated as constant in the low-temperature region of interest. We believe that our assumption is quite realistic. However, over a larger range of temperature this approximation could fail.

Applying a static magnetic field parallel to the c axis of the crystal, we may in the usual approximation substitute in Eq. (1) directly

$$k_z^2 = (2/\lambda^2)(\tilde{\alpha} + \frac{1}{2}), \quad \lambda^2 = \hbar/eB, \quad \tilde{\alpha} = 0, 1, 2, \dots \quad (2)$$

The model W2 leads to equidistant Landau levels but in W1 and J the energy separation of the Landau levels decreases with increasing k_z^2 , with model W1 showing the stronger tendency.

In both models W1 and J the joint density of states has only one relevant singularity which is at $k_z = 0$. The occupation probability, however, suppresses at low temperatures this singularity so that the optical transitions between Landau levels take place at the valence-band maximum, that is, at $|k_z| = k_m$. This result agrees with that of Bangert and Dreybrodt.²²

V. CALCULATION OF ABSORPTION CONSTANT

The complex dielectric constant is related to the complex frequency-dependent conductivity by

$$\epsilon(\omega) = \epsilon_0(n^2 - \kappa^2 + 2in\kappa) = \epsilon_i + i\sigma(\omega)/\omega, \quad (3)$$

where n and κ are the refractive and absorption indexes, respectively, ϵ_i is the lattice part of the dielectric constant, ϵ_0 is the dielectric constant of the vacuum, $\sigma(\omega)$ is the complex conductivity, and ω is the radiation frequency.

The real part of the conductivity is a direct measure for the absorption index κ because the change in refractive index is negligible for $p = 4 \times 10^{13} \text{ cm}^{-3}$ in this frequency range. To calculate the magnetic-field-dependent part of the conductivity we apply Kubo's general formula²³

$$\sigma_{\mu\nu}(\omega) = (1/V) \int_0^\infty dt e^{-i\omega t} \int_0^\beta d\lambda \langle J_\nu(-i\hbar\lambda) J_\mu(t) \rangle. \quad (4)$$

TABLE II. List of band parameters.

Parameter	Model W1	Model W2	Model J
a	0.06315 eV	0.06315 eV	0.06315 eV
b	$-11.0\hbar^2/m_0$	$-10.1\hbar^2/2m_0$	$-4.0 \times 10^{-15} \text{ eV cm}^2$
c	$-5.55\hbar^2/2m_0$	$-9.95\hbar^2/2m_0$	$-2.6 \times 10^{-15} \text{ eV cm}^2$
d	$0.3 \times 10^{-28} \text{ eV cm}^4$	$1.1 \times 10^{-28} \text{ eV cm}^4$	$0.63 \times 10^{-28} \text{ eV cm}^4$
e	$0.2 \times 10^{-28} \text{ eV cm}^4$	0	0
f	$-5.55\hbar^2/2m_0$	0	$-1.32 \times 10^{-15} \text{ eV cm}^2$
g	0	0	$-0.42 \times 10^{-29} \text{ eV cm}^4$
h	$0.0618 \times 10^{-14} (\text{eV cm})^2$	$0.0625 \times 10^{-14} (\text{eV cm})^2$	$0.0676 \times 10^{-14} (\text{eV cm})^2$

Here J_ν and J_μ are the current operators, $\beta = 1/kT$, and V is the normalization volume. The time dependence of the operators is specified by

$$J(t) = e^{+i\mathcal{H}t/\hbar} J e^{-i\mathcal{H}t/\hbar}, \quad (5)$$

where \mathcal{H} is the Hamiltonian of the total system. The angular brackets $\langle \rangle$ indicate the average over the thermodynamical equilibrium distribution. Starting with the conductivity formula of Eq. (4), we neglect magnetic transitions and have chosen the interaction operator between particles and radiation field of the form

$$\mathcal{H}_{\text{inter}} = \sum_\nu e \vec{r}_\nu \cdot \vec{E}(t). \quad (6)$$

This particular choice of the interaction operator is quite important because (6) is the only form of the interaction which avoids an approximated mass parameter as, for example, is found in the calculations of Apel *et al.*²⁴ and Bangert and Dreybrodt.²² Reliable results considering nonparabolic effects are only obtained without these approximations. For the real part of the conductivity, Eq. (4) reduces to²⁵

$$\text{Re}\sigma_\pm(\omega) = \frac{1 - e^{-\beta\hbar\omega}}{\hbar\omega V} \text{Re} \int_0^\infty dt \langle J_\mp J_\pm(t) \rangle e^{-i\omega t}. \quad (7)$$

Here the current operators J_\pm are defined as

$$J_\pm = (J_x \mp iJ_y) / \sqrt{2} \quad (8)$$

because we are interested in the absorption of circular polarized light. In the following we adopt the one-electron picture by assuming that the electron-electron interaction is considered in the one-electron band and in a scattering potential U . On these assumptions the right-hand side of Eq. (7) can be written in one-electron expressions

$$\text{Re}\sigma_\pm(\omega) = \frac{1 - e^{-\beta\hbar\omega}}{\hbar\omega V} \text{Re} \int_0^\infty dt e^{-i\omega t} \times \text{Tr} \{ f(\mathcal{H}) J_\mp [1 - f(\mathcal{H})] J_\pm(t) \}. \quad (9)$$

Here $f(\mathcal{H})$ is the Fermi-Dirac distribution function. The one-electron Hamiltonian \mathcal{H} consists of the unperturbed kinetic energy \mathcal{H}_0 defined by the detailed $E(k)$ dependence and the potential energy U representing the interaction with the scatterers.

Considering the influence of the scattering potential, we follow Kawabata²⁵ and take into account only its influence in form of a damping denominator replacing the usual δ function. Thus we have

$$\begin{aligned} \text{Re}\sigma_+(\omega) &= \frac{1 - e^{-\beta\hbar\omega}}{\omega V} \\ &\times \text{Re} \sum_\alpha f(E_\alpha) [1 - f(E_{\alpha+1})] \langle \alpha | J_- | \alpha + 1 \rangle \\ &\times \frac{\langle \alpha + 1 | J_+ | \alpha \rangle}{i[\hbar\omega - (E_{\alpha+1} - E_\alpha)] + \Gamma}, \quad (10) \end{aligned}$$

where Γ is, in general, a function of both ω and the magnetic field. In this paper, however, we treat Γ as a constant parameter being affected only by the temperature as determined experimentally. In Eq. (10) we took account of the selection rules by the matrix elements. Here α and $\alpha + 1$ represent the sets of quantum numbers $\tilde{\alpha}$, X , k_x and $\tilde{\alpha} + 1$, X , k_x , respectively. Thus the summation \sum_α is actually a triple sum running explicitly over $\tilde{\alpha}$, X , and k_x . Making the additional approximation of

$$e^{-\beta\hbar\omega} \approx e^{-\beta(E_{\alpha+1} - E_\alpha)} \quad (11)$$

which evidently holds well in the vicinity of the absorption peak, we can reduce Eq. (10) to

$$\text{Re}\sigma_+ = \text{Re} \frac{1}{\omega V} \sum_\alpha \frac{[f(E_\alpha) - f(E_{\alpha+1})] |J_{\pm, \alpha, \alpha+1}|^2}{i[\hbar\omega - (E_{\alpha+1} - E_\alpha)] + \Gamma}. \quad (12)$$

This expression agrees with the result of Kawabata²⁵ in so far as we have not approximated $1/\hbar\omega$ by $1/(E_{\alpha+1} - E_\alpha)$. This form of frequency and magnetic field dependence of Eq. (12) is in agreement with the result of Apel *et al.*²⁴ These authors, however, replaced the summation over the center coordinates

$$\sum_X = \frac{L}{2\pi\lambda^2} \int_0^L dX = \frac{eBL^2}{2\pi\hbar} \quad (13)$$

by

$$\sum_X = \frac{L^2(E_{\alpha+1} - E_\alpha) m}{2\pi\hbar^2},$$

which no longer holds in the nonparabolic case.

Using the relation

$$\vec{J} = e\dot{\vec{r}} = (ie/\hbar)[\mathcal{H}_0, \vec{r}], \quad (14)$$

we take into account the important difference between the kinetic and the canonical momentum in the nonparabolic problem, which has not been considered by Bangert and Dreybrodt²²:

$$\begin{aligned} \text{Re}\sigma_+(\omega) &= \text{Re} \frac{e}{\hbar\omega VB} \\ &\times \sum_\alpha \frac{[f(E_\alpha) - f(E_{\alpha+1})] (E_{\alpha+1} - E_\alpha)^2 (\tilde{\alpha} + 1)}{i[\hbar\omega - (E_{\alpha+1} - E_\alpha)] + \Gamma}. \quad (15) \end{aligned}$$

For a parabolic $E(k)$ relation, Eq. (15) reduces to

$$\begin{aligned} \text{Re}\sigma_+(\omega) &= \frac{\text{Re} e}{\hbar\omega VB m^2} \\ &\times \sum_\alpha \frac{[f(E_\alpha) - f(E_{\alpha+1})] e^2 B^2 \hbar^2 (\tilde{\alpha} + 1)}{i(\hbar\omega - eB\hbar/m) + \Gamma}. \quad (16) \end{aligned}$$

In the quantum limit the magnetic field B_m of the absorption maximum shows for constant-carrier concentration a definite dependence on the damping parameter

$$B_m = (m/e)(\omega^2 + \Gamma^2/\hbar^2)^{1/2} \quad (17)$$

Thus even for the parabolic problem we should expect a shift of the absorption line to higher magnetic fields with increasing temperature owing to the generally growing value of Γ with increasing temperature.

After adaption to *p*-type carriers, we computed Eq. (15) under the restriction of a constant number of carriers for different temperatures and took into account the detailed structure of the band models W1, W2, and J. In the computation we approximated the Fermi-Dirac distribution function by the Boltzmann function, which is a good approximation for the hole concentration of $4 \times 10^{13} \text{ cm}^{-3}$ in the temperature range considered.

VI. DISCUSSION OF THEORETICAL RESULTS

In Fig. 8 we have plotted the magnetic-field-dependent part of the absorption constant for each of the three models discussed so far as a function of the magnetic field \vec{H} , assuming the susceptibility in Te being $\mu = 1$. As the parameter we have chosen the radiation wavelength of $337 \mu\text{m}$ and three different temperatures of the low-, intermediate-, and high-temperature range. As the damping constant we have chosen the small value of 0.1 meV which yields an $\omega\tau$ of about 37.

Despite former predictions,^{9,10} the absorption constant computed with W1 and J shows no splitting as a function of the magnetic field even at high temperatures. Actually the singularity in the joint density of states at $k_z = 0$ is so weak that it is completely obscured by the influence of the occupation probability which allows transitions only in the direct vicinity of the band extrema at $|k_z| = k_m$ at low temperatures. This result agrees with that of Bangert and Dreybrodt.²² With increasing temperature more states of large $|k_z|$ and heavier transverse mass are occupied, as can be seen by the smoothly decreasing slope in higher magnetic fields.

Model W2 shows a detailed structure in the absorption constant. As a matter of fact this is not surprising because for the parallel Landau levels in this model the joint density of states has strong singularities for each time being equal to the difference of two adjacent Landau levels. Particularly in the absorption constant of this model we can observe the influence of the matrix elements which favors the transitions with large quantum numbers.

In Figs. 2-7 we have plotted the magnetic field required for peak absorption as a function of temperature for two different damping parameters which are close to our experimental values. Whereas the curves for model W2 show a very strong and steady increase with temperature, the curves for model W1 contain a pronounced minimum and the curves for model J show a similar tendency. This

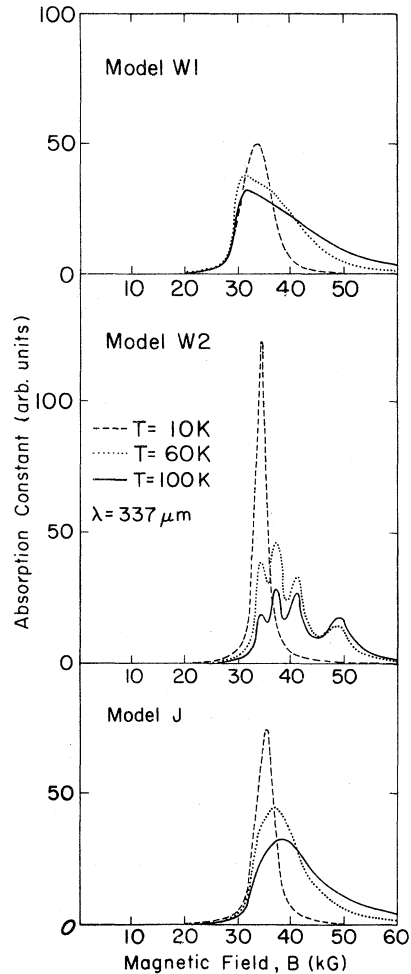


FIG. 8. Magnetic-field-dependent part of absorption constant for $337\text{-}\mu\text{m}$ radiation calculated as a function of the magnetic field for $\Gamma = 0.1 \text{ meV}$ and $\lambda = 337 \mu\text{m}$.

minimum follows directly from the nonequidistant separation of the Landau levels. At low temperature only hole states near $|k_z| = k_m$ are occupied. With slowly increasing temperature the branch with $|k_z| < k_m$ has a greater influence on the cyclotron-resonance absorption than the branch with $|k_z| > k_m$ because of the approach toward the singularity in the joint density of states at $k_z = 0$. At still increasing temperature, higher Landau levels are populated which suppress the first effect. The influence of the nonparallelism is very strong in model W1 which causes a definite minimum in the temperature dependence of the peak position. The damping parameter Γ which is usually increasing with temperature may, however, counteract and shift the peak position to higher magnetic fields. Therefore, a minimum or even a plateau in the temperature variation of the peak position of the absorption constant is a definite indication for non-

parallel Landau levels as function of k_x , whereas the absence of that minimum is not yet a sufficient criterion for parallel levels, as can be seen in Figs. 4 and 7.

VII. COMPARISON OF THEORY AND EXPERIMENTAL RESULTS

Contrary to Bangert and Dreybrodt,²² we believe that the differences in the line shape and in the peak position that we have calculated from these three models are sufficiently pronounced to test the models in comparison with our experimental data. These differences are as large as 6% for the data taken at a wavelength of 220 μm . Such a comparison has suggested to us the relative usefulness of each model. For example, we have compared the line shape of our experimental data with the shape predicted by model W1. Although we do not obtain a perfect fit, this model provides the best agreement in line position and line shape with our experimental results as can be seen in Figs. 2, 5, and 9. Figures 3, 4, 6, and 7 show that the comparison of the low-temperature data for line position with models W2 and J is not as favorable. It would be difficult, however, to reject model J totally were it not for the line-shape results shown in Fig. 9. Figure 9 shows the line shape calculated from W1, in comparison with that of a typical measurement using circularly polarized 220- μm radiation. As the fitting parameter, we used a damping constant of $\Gamma = 0.8$ meV. Because of the assumption of a field-independent Γ , we are not able to fit the line over the entire field range. We obtained the temperature dependence of the damping parameter as shown in Fig. 10 by doing this analyzing procedure for each of the measurements with polarized light. This function happens to be independent of the laser frequency ω . As a function of temperature, $\Gamma = \text{const} \times T^{0.375}$. This functional dependence may be interpreted as being due to a superposition of different scattering mechanisms. Applying this function $\Gamma(T)$ we computed the mag-

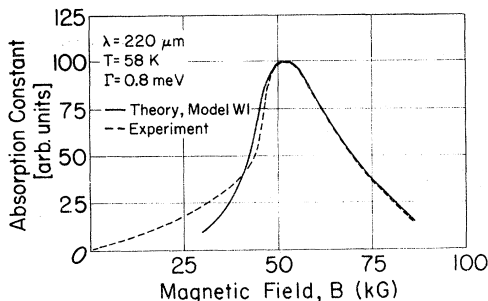


FIG. 9. Magnetic-field-dependent part of absorption constant for 220- μm radiation in tellurium as a function of the magnetic field. Theory based on model W1.

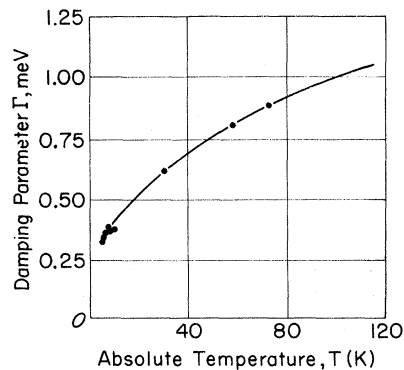


FIG. 10. Damping parameter derived from cyclotron-resonance measurements in tellurium as a function of temperature.

netic field of the peak position in model W1 as shown by the solid curves in Figs. 2 and 5. The agreement between theory and experiment is rather good, particularly for the 337- μm radiation as can be seen in Fig. 5. Whereas model W2 in Figs. 3 and 6 and model J in Figs. 4 and 7 show no minimum of the line position, model W1 shows a pronounced minimum at low temperatures. Indeed, for $\Gamma = \Gamma(T)$, the minimum calculated from W1 is more pronounced than that of the experimental data. The agreement between theory and experiment for the 220- μm line is worse, as can be seen in Fig. 2. Whereas W1 predicts a pronounced minimum, models J and W2 produce none if the temperature dependence of Γ is included. As a matter of fact, both these models show a monotonic, rather strong increase in the low-temperature range of interest. We think that in model J the influence of the k^4 term is too dominant and that the nonequidistant separation of the Landau levels should be more pronounced, whereas in model W1 we find the opposite. Model W2 shows the strongest monotonic shift of the line position to higher magnetic fields with increasing temperature. Because of this fact it has the worst agreement with our experimental results in the low-temperature region, which is critical for our comparison as shown later on.

The minimum in the experimental data at 220 μm is actually more like a plateau. However, even this plateau is a strong evidence for nonparallel Landau levels as stated in Sec. VI. This conclusion remains unaffected by a possible temperature dependence of the band parameters, because the results of Anzin *et al.*²⁰ support either an increasing minimum in the camel back or an increasing transverse mass with rising temperature. Neither effect is able to produce the experimentally proved minimum in the absorption line position of 337- μm radiation as a function of tem-

perature.

We based our comparison between experiment and theory mainly on the low-temperature data, because at high temperatures the temperature dependence of the band parameters should not be neglected any more. In addition, at higher temperatures states of large k are occupied and the models are no longer realistic because of the limitation to terms of k^4 . Therefore a new model should include higher-order terms in k to avoid a second extremum in the band structure. Also we have neglected the influence of coupling between holes and LO phonons in higher Landau levels.¹¹ The hole-LO-phonon coupling in lower levels may be neglected because the LO-phonon energy is 13 meV.²⁶ In conclusion we state that from comparison of our experimental data with the theoretical results based on the models W1, W2, and J, the Landau levels in Te are not equidistant as a function of k_z .

For the purpose of defining the different parameters of the entire band-structure model more completely, we are now repeating the cyclotron-resonance measurements with pure samples for the transverse orientation $\vec{H} \perp \vec{c}$. We conclude at this point, however, that a more satisfactory k_z dependence must still be formulated in a model that lies between W1 and J but closer to W1. We also emphasize that any comparison of experimental data concerning cyclotron-resonance mass and peak positions is only meaningful together with an analyzing procedure including temperature dependence and linewidth.

But even by trying this in extrapolation, our

measurements are in disagreement with the low-temperature data published by Yoshizaki and Tanaka.¹⁰ Additional measurements with the 195- μm line of a DCN laser confirms that our line position is always at lower magnetic field values.

VIII. SUMMARY

We have observed cyclotron-resonance absorption in pure p -type Te showing no impurity absorption lines. The measurements were carried out with laser wavelengths of 220 and 337 μm as function of temperature from 5 to 120 K. We compared our experimental results with the theoretical absorption taking the detailed structure of three competitive models W1,¹³ W2,⁹ and J¹⁰ into account. We found the best agreement with model W1, which was fairly good. From comparisons of both line shape and temperature dependence with theory, we can state that there are no equidistant Landau levels as a function of k_z in Te. In particular, the controversy concerning a splitting of the cyclotron-resonance line owing to transitions at $k_z = 0$ and $|k_z| = k_m$ should have been resolved now because such a splitting is not present in the experimental data for these pure specimens. Also the theory predicts no splitting because of the weakness of the singularity in the joint density of states at $k_z = 0$.

ACKNOWLEDGMENTS

We would like to thank E. Sudenfield for technical assistance and E. Taylor for typing the manuscript.

*Supported by Max Kade Foundation, New York, N. Y., on leave of absence from Physikalisches Institut der Universität Würzburg, Germany. Author wishes to express his gratitude to the Max Kade Foundation for financial support.

†Supported by the National Science Foundation.

‡Supported by Deutsche Forschungsgemeinschaft, Germany.

¹O. Betbeder-Matibet and M. Hulin, Phys. Status Solidi **36**, 573 (1969).

²T. Doi, K. Nakao, and H. Kamimura, J. Phys. Soc. Japan **28**, 36 (1970).

³T. Doi, K. Nakao, and H. Kamimura, J. Phys. Soc. Japan **28**, 822 (1970).

⁴K. Nakao, T. Doi, and H. Kamimura, J. Phys. Soc. Japan **30**, 1400 (1971).

⁵P. L. Radoff and R. N. Dexter, Bull. Am. Phys. Soc. **14**, 330 (1969).

⁶Y. Couder, Phys. Rev. Letters **22**, 890 (1969).

⁷K. J. Button, G. Landwehr, C. C. Bradley, P. Grosse, and B. Lax, Phys. Rev. Letters **23**, 14 (1969).

⁸W. Dreybrodt, K. J. Button, and B. Lax, Solid State Commun. **8**, 1021 (1970).

⁹W. Dreybrodt, M. H. Weiler, K. J. Button, B. Lax, and G. Landwehr, in *Proceedings of the Tenth Inter-*

national Conference on the Physics of Semiconductors, Cambridge, Mass., 1970 (U. S. AEC, Division of Technical Information, Springfield, Va., 1970), p. 347.

¹⁰R. Yoshizaki and S. Tanaka, J. Phys. Soc. Japan **30**, 1389 (1971).

¹¹K. J. Button, D. R. Cohn, M. H. Weiler, B. Lax, and G. Landwehr, Phys. Letters **35A**, 281 (1971).

¹²K. F. Renk, Solid State Commun. **9**, 1175 (1971).

¹³M. H. Weiler, Solid State Commun. **8**, 1017 (1970).

¹⁴K. J. Button and B. Lax, in *Submillimeter Waves* (Polytechnic Press of the Polytechnic Institute of Brooklyn, New York, 1971), pp. 401-416; K. J. Button, in *Optical Properties of Solids*, edited by E. D. Haide-menakis (Gordon and Breach, New York, 1970), pp. 253-279; Laser Focus **7**, No. 8, 29 (1971).

¹⁵K. J. Button, B. Lax, and D. R. Cohn, Phys. Rev. Letters **24**, 375 (1970).

¹⁶T. L. Cronburg and B. Lax, Phys. Letters **37A**, 135 (1971).

¹⁷D. Fischer and P. Grosse, Phys. Status Solidi **44**, kl33 (1971).

¹⁸E. Bangert and M. v. Ortenberg (unpublished).

¹⁹P. Gspan, R. Drope, and P. Grosse, Verhandl. DFG (VI) **5**, 286 (1970).

²⁰V. B. Anzin, Yu. V. Kosichkin, V. G. Veselago, P.

N. Lebedev, I. I. Farbstein, S. S. Shalyt, E. S. Itskevich, and V. A. Sukhopavov, International Colloquium GNRS, Report No. 188, Grenoble, 1970, p. 143 (unpublished).

²¹V. B. Anzin, M. S. Bresler, I. I. Farbstein, E. S. Itskevich, Yu V. Kosichkin, V. A. Sukhopavov, A. S. Telepnev, and V. G. Veselago, Phys. Status Solidi **48**, 531 (1971).

²²E. Bangert and W. Dreybrodt, Solid State Commun. **10**, 623 (1972).

²³R. Kubo, J. Phys. Soc. Japan **12**, 570 (1957).

²⁴J. R. Apel, T. O. Poehler, C. R. Westgate, and R. I. Joseph, Phys. Rev. B **4**, 2 (1971).

²⁵A. Kawabata, J. Phys. Soc. Japan **23**, 999 (1967).

²⁶M. Selders and P. Grosse (private communication).

PHYSICAL REVIEW B

VOLUME 6, NUMBER 6

15 SEPTEMBER 1972

Optical Properties of K between 4 and 10.7 eV and Comparison with Na, Rb, and Cs[†]

U. S. Whang* and E. T. Arakawa

Health Physics Division, Oak Ridge National Laboratory, Oak Ridge, Tennessee 37830

and

T. A. Callcott[‡]

Department of Physics, The University of Tennessee, Knoxville, Tennessee 37916

(Received 13 March 1972)

The optical and dielectric constants of K have been determined from reflectance and transmission measurements for photons of energy between 4.0 and 10.7 eV. Reflectance measurements were made as a function of incident angle at a K-MgF₂ interface in an ultrahigh-vacuum system. The refractive index (n) was determined from the critical angle for total internal reflection and the absorption coefficient (k) from the slope of the reflectance curve at the critical angle and from transmission measurements. The real part of the dielectric function (ϵ_1) and the optical conductivity $\sigma = \omega \epsilon_2 / 4\pi$ were derived from n and k . In σ we find a broad peak centered at 8 eV. This absorption peak is discussed along with comparable peaks in Na, Rb, and Cs. One-electron and many-body processes that might give absorption in this energy region are discussed. ϵ_1 is analyzed in terms of a nearly-free-electron model to obtain a value of the effective mass (m_{eff}) and of the contribution of core polarization ($4\pi n_0 \alpha$) to ϵ_1 . We find $4\pi n_0 \alpha = 0.15 \pm 0.01$ and $m_{\text{eff}}/m_0 = 1.01 \pm 0.01$.

INTRODUCTION

This is the last of a series of papers¹⁻³ by the present authors reporting measurements of the optical properties of the alkali metals Cs, Rb, and K for photons of energy between 3.5 and 11 eV. Similar measurements have been reported by Sutherland and Arakawa⁴ for Na. Optical measurements on these metals at energies below the plasma frequency give results in fair agreement with a nearly-free-electron (NFE) model that includes the effects of free-carrier absorption and interband transitions between the filled conduction band and the next-higher band.⁵⁻⁷

Our measurements clearly show the existence of an additional absorption process in all of the alkalis at energies above the plasma frequency. In previous papers, broad strong absorption peaks in the optical conductivity have been reported in Cs and Rb with maxima at 5 and 6.8 eV, respectively. A weaker peak is centered at 10 or 11 eV in Na.

This paper is divided into two parts. In the first part, we report experimental determinations of the

index of refraction (n), the absorption coefficient (k), the real and imaginary parts of the dielectric response function (ϵ_1 and ϵ_2), and the optical conductivity (σ) of K for photon energies of 3.3 to 10.7 eV. In σ , we find a broad absorption peak centered at 8 eV that is similar to the peaks observed in the other alkalis. A Kramers-Kronig analysis applied to $\epsilon_2 = 4\pi\sigma/\omega$ is used to calculate the effect of interband transitions and of the broad high-energy peak on ϵ_1 . When these contributions are subtracted, the remaining portion of ϵ_1 represents that expected for a NFE model containing only free-carrier absorption. These corrected values of ϵ_1 are used to obtain values of the effective mass and of the core polarization, which are the adjustable parameters of such a free-electron model.

In the second part of the paper, we briefly summarize the optical properties of all of the alkali metals between Na and Cs for photon energies above their plasma frequencies. Plots are given of σ for these four materials. The broad absorption peaks in σ are found to become stronger and move to lower energies for alkali metals of larger atomic num-